NANO · MICRO small
www.small-journal.com

Active Encapsulation in Biocompatible Nanocapsules

Baiheng Wu, Chenjing Yang, Bo Li, Leyun Feng, Mingtan Hai, Chun-Xia Zhao, Dong Chen, Kai Liu,* and David A. Weitz*

Co-precipitation is generally refers to the co-precipitation of two solids and is widely used to prepare active-loaded nanoparticles. Here, it is demonstrated that liquid and solid can precipitate simultaneously to produce hierarchical core–shell nanocapsules that encapsulate an oil core in a polymer shell. During the co-precipitation process, the polymer preferentially deposits at the oil/water interface, wetting both the oil and water phases; the behavior is determined by the spreading coefficients and driven by the energy minimization. The technique is applicable to directly encapsulate various oil actives and avoid the use of toxic solvent or surfactant during the preparation process. The obtained core–shell nanocapsules harness the advantage of biocompatibility, precise control over the shell thickness, high loading capacity, high encapsulation efficiency, good dispersity in water, and improved stability against oxidation. The applications of the nanocapsules as delivery vehicles are demonstrated by the excellent performances of natural colorant and anti-cancer drug-loaded nanocapsules. The core–shell nanocapsules with a controlled hierarchical structure are, therefore, ideal carriers for practical applications in food, cosmetics, and drug delivery.

1. Introduction

Nanocapsules have attracted much attention in chemistry, material, medicine, pharmacology, and nanotechnology because of their wide-range applications in catalysis, intelligent textile, medical diagnostics, drug delivery, and functional food.[1–13] Hierarchical core–shell nanocapsules are promising carriers that could encapsulate various oil actives in a polymer shell, protect them from harsh ambient conditions and release them when it is required.[14–19] Encapsulation of the oil actives in the nanocapsules can effectively alleviate their deficiencies of low stability and poor dispersity in water, thus increasing their bioavailability.[20] For example, many food active molecules, such as antioxidants and aromas, exist in an oil form and effective encapsulation of the oils in the core of nanocapsules is generally required for practical applications.[21,22]

To meet the demands, a variety of techniques have been developed to prepare core–shell nanocapsules that consist of an inner oil core surrounded by a polymer shell.[23–26] They can be divided into chemical methods, such as complex coacervation,[27,28] interfacial polymerization,[29] and polymerization induced phase separation,[30] and physical methods, such as fluid bed coating,[31] one-step emulsification,[32–34] and two-step emulsification.[35] Despite the significant advances, the widespread applications of nanocapsules are limited by the use of toxic solvent or surfactant (cause foaming), disqualifying the resulting materials from being used in food, cosmetic, and drug delivery. Thus, encapsulation of various oil actives in biocompatible core–shell nanocapsules using all FDA-approved materials remains an important but challenging task.[36] Innovations of technologies for the green preparation of biocompatible nanocapsules with controlled hierarchical structure and property are essential.

Here, we develop a facile method to actively encapsulate various oils in the biocompatible core–shell nanocapsules. By virtue of controlled co-precipitation under rapid mixing, small oil molecules aggregate first to form oil droplets while shellac polymer subsequently precipitates at the oil/water interface to minimize the total free energy, forming core–shell nanocapsules. To demonstrate the application of the oil-core nanocapsules as delivery vehicles, we use capsanthin, a hydrophobic natural colorant, as our model cargo. The prepared capsanthin-loaded nanocapsules are well dispersed in water and are able

Dr. B. Wu, C. Yang, L. Feng, Prof. D. Chen
Institute of Process Equipment
College of Energy Engineering
Zhejiang University
Zheda Road No. 38, Hangzhou 310027, China
E-mail: chen_dong@zju.edu.cn
Dr. B. Wu, Prof. D. Chen
State Key Laboratory of Fluid Power and Mechatronic Systems
Zhejiang University
Zheda Road No. 38, Hangzhou 310027, China
B. Li, Prof. K. Liu
Changchun Institute of Applied Chemistry
Chinese Academy of Sciences
Changchun 130022, China
E-mail: kai.liu@ciac.ac.cn
Prof. M. Hai, Prof. C.-X. Zhao, Prof. D. Chen, Prof. K. Liu, Prof. D. A. Weitz
John A. Paulson School of Engineering and Applied Sciences
Harvard University
Cambridge, MA 02138, USA
Prof. C.-X. Zhao
Australian Institute for Bioengineering and Nanotechnology
The University of Queensland
St Lucia, QLD 4072, Australia
The ORCID identification number(s) for the author(s) of this article can be found under https://doi.org/10.1002/smll.202002716.

DOI: 10.1002/smll.202002716

to protect capsanthin from destructive environmental factors, substantially improving its stability. Since the nanocapsules are prepared in the absence of any chemical reactions and using all FDA-approved materials and non-toxic solvents, the hierarchical core–shell nanocapsules are well suited for practical applications in food, cosmetic, and drug delivery.

2. Results and Discussions

To synthesize the core–shell nanocapsules, we use shellac polymer, an FDA-approved natural resin mainly consisted of a mixture of polyesters and single esters (Figure S1, Supporting Information),[37] as our shell material and use vegetable oil, in which many hydrophobic active ingredients have a fair solubility, as our inner core. Capsanthin, the principal red coloring compounds of paprika oleoresin (**Figure 1**a),[38] is used as the model active ingredient and loaded in the nanocapsules to demonstrate their applications as delivery vehicles. Capsanthin barely dissolves in ethanol, while a small amount of vegetable oil could significantly increase its solubility in ethanol, as shown in the inset of Figure 1a. Therefore, capsanthin, vegetable oil, and shellac polymer are co-dissolved in the ethanol solution. To prepare the nanocapsules, we quickly inject the ethanol solution into a water reservoir using a small microcapillary tip to ensure rapid mixing. Upon sudden solvent exchange, vegetable oil and shellac polymer co-precipitate while shellac polymer preferentially deposits at the periphery of the oil droplets, forming core–shell nanocapsules, as modeled in Figure 1b. The capsanthin-loaded nanocapsules are well dispersed in water while capsanthin imparts a vivid color to the solution, as shown in Figure 1c and modeled in Figure 1d. When the oil cores are removed, collapsed polymer shells of the nanocapsules are characterized by the SEM image, as shown in Figure 1e.

We propose that the co-precipitation process involves three steps: i) rapid mixing leads to the sudden solvent exchange and the co-precipitation of vegetable oil and shellac; ii) small vegetable oil molecules aggregate first to form oil droplets, as vegetable oil has a smaller molecular weight and thus a larger molecular mobility; iii) shellac polymer subsequently precipitates at the oil/water interface to minimize the total energy, as schematically illustrated in **Figure 2**a. Similar to the rapid mixing in microfluidic channels, when the ethanol solution is quickly injected into a water reservoir using a small

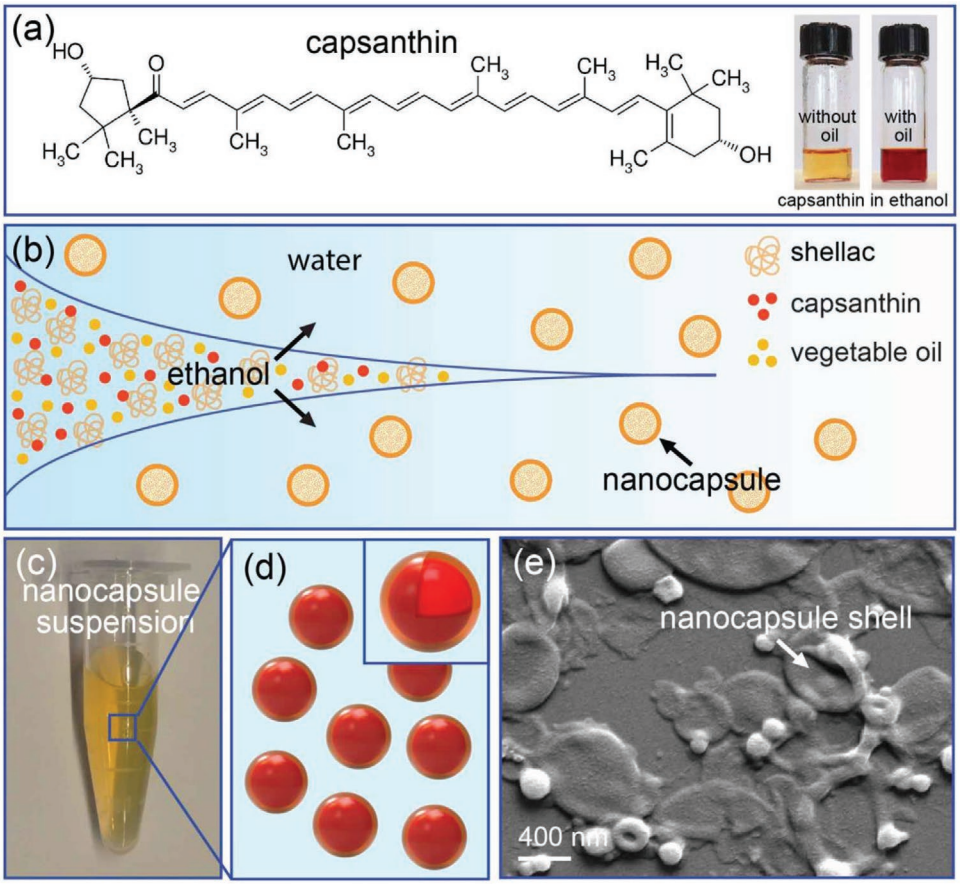

Figure 1. Controlled preparation of hierarchical core–shell nanocapsules by co-precipitation upon rapid mixing. a) Chemical structure of capsanthin, a natural red carotenoid. Capsanthin barely dissolves in ethanol, while a small amount of vegetable oil could significantly increase its solubility in ethanol, imparting a dark red color, as shown in the insets. b) Schematic illustration of the formation of nanocapsules. Upon solvent diffusion, shellac polymer preferentially precipitates at the periphery of oil droplets, forming core–shell nanocapsules. c) Stable suspension of capsanthin-loaded nanocapsules after 48 days stored in dark at room temperature and modeled in (d). e) SEM image showing collapsed thin shells of nanocapsules after removing the oil cores using ethyl acetate.

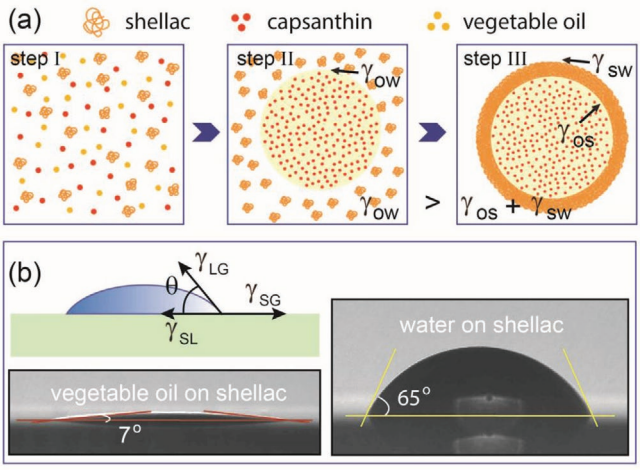

(c) γ_{ow} (22 mN/m) > γ_{os} (4 mN/m) + γ_{sw} (6 mN/m)

	γ_{SG}	γ_{LG}	θ	γ_{SL}
water	36 mN/m	72 mN/m	65°	6 mN/m
vegetable oil	36 mN/m	32 mN/m	7°	4 mN/m

Figure 2. Self-assembly of core–shell nanocapsules driven by energy minimization. a) Three-step formation of nanocapsules: i) rapid solvent exchange, ii) small oil molecules form oil droplets first, and iii) shellac polymer subsequently precipitates at the interface. b) Calculation of γ_{SL} by Young's equation $\gamma_{SL} = \gamma_{SG} - \cos\theta\gamma_{LG}$, where γ_{SL}, γ_{SG}, and γ_{LG} are the solid/liquid, solid/gas, and liquid/gas interfacial tensions, respectively. The solid/gas interfacial tension γ_{SG} is obtained from the literature.[45] c) Calculation of the spreading coefficient $S = \gamma_{ow} - (\gamma_{os} + \gamma_{sw}) > 0$, suggesting that the replacement of the oil/water interface with the water/shellac and oil/shellac interfaces lowers the total energy, where γ_{ow}, γ_{os}, and γ_{sw} are the oil/water, oil/shellac, and shellac/water interfacial tensions, respectively. The oil/water interfacial tension γ_{ow} is measured by pendent drop experiments.

microcapillary pipette tip, the mixing time τ_{mix} of ethanol with water (around 10 ms)[39] could be shorter than the typical polymer aggregation time τ_{agg} (around 30 ms).[40,41] Therefore, both vegetable oil and shellac polymer experience a rapid exchange of solvent, leading to their co-precipitation. In general, there are four possible morphologies for the two-phase system: core–shell, occluded, acorn and heteroaggregate, while the final morphology is determined by the energy minimum and could be predicted by the spreading coefficients.[42–45] To calculate the spreading coefficients, the interfacial tension of solid and liquid is derived from Young's equation, $\gamma_{SL} = \gamma_{SG} - \cos\theta\gamma_{LG}$, where γ_{SL}, γ_{SG}, and γ_{LG} are the solid/liquid, solid/gas, and liquid/gas interfacial tensions, respectively, as shown in Figure 2b; we obtain $\gamma_{os} \approx 4$ mN m^{-1} and $\gamma_{sw} \approx 6$ mN m^{-1}, where γ_{os} and γ_{sw} are the oil/shellac and shellac/water interfacial tensions, respectively. The oil/water interfacial tension γ_{ow} measured by pendent drop experiments is $\gamma_{ow} \approx 22$ mN m^{-1} and we get $S_1 = \gamma_{ow} - (\gamma_{os} + \gamma_{sw}) > 0$, $S_2 = \gamma_{os} - (\gamma_{ow} + \gamma_{sw}) < 0$, and $S_3 = \gamma_{sw} - (\gamma_{os} + \gamma_{ow}) < 0$. Therefore, shellac polymer tends to lower the total energy and precipitate at the oil/water interface, forming a core–shell structure, as shown in Figure 2c. The tendency of shellac polymer to wet both oil and water benefits from its chemical compositions, containing both hydrophobic ester groups and hydrophilic carboxyl groups. Therefore, controlling the co-precipitation behavior under rapid mixing and directing the self-assembly of polymer at the oil/water interface provide a simple and green way to prepare biocompatible core–shell nanocapsules.

To demonstrate the flexible tailoring of the size and shell thickness of the nanocapsules, we follow the same procedure and prepare a series of different nanocapsules using 25/25, 25/50, and 25/100 μL mg^{-1} solutions. The notion 25/50 μL mg^{-1} denotes 25 μL vegetable oil and 50 mg shellac polymer per mL ethanol. When the amount of vegetable oil is kept constant at 25 μL per mL ethanol, the size of the nanocapsules measured by light scattering slightly increases as the concentration of shellac polymer increases while the zeta potential is roughly the same, as shown in **Figure 3**a,b and Figure S2, Supporting Information. The results are consistent with the co-precipitation scenario that small vegetable oil molecules aggregate first to form oil droplets while shellac polymer subsequently deposits at their periphery. When the concentration of vegetable oil is kept constant, the oil cores have roughly a same size. As the concentration of shellac polymer increases from 25 to 100 mg per mL ethanol, the shell thickness, $t = r - r_0 = (\sqrt[3]{1+\varphi} - 1)r_0$ increases from $t \approx 31$ to ≈56 nm if we assumed the oil cores have an average size of $r_0 \approx 150$ nm as estimated from the light scattering results in Figure 3a and the SEM images in Figure 3c–e, thus contributing to a small increase in the nanocapsule size, where r, is the radius of the nanocapsules and φ, is the volume ratio of shellac to oil. The increase in shell thickness also enhances the rigidity of the shells, that is, thin shells collapse when the oil cores are removed while thick shells retain their spherical shape, as characterized by their morphology shown in Figure 3c–e and modeled in the insets. When the concentration of shellac is kept constant at 50 mg mL^{-1}, the size of the nanocapsules slightly increases as the concentration of oil increases, as shown in Figure S3, Supporting Information. When we reduce the concentration of oil to 5 μL per mL and the concentration of shellac to 5 mg mL^{-1}, we obtain nanocapsules as small as 125 ± 58 nm.

The versatile method of making biocompatible core–shell nanocapsules is applicable to encapsulate various oils, such as vitamin E, rosemary oil, and jasmine oil, as shown in **Figure 4**a–c, respectively. The shell material could be varied from shellac polymer to other biocompatible polymers, which are soluble in ethanol and contain both hydrophilic and hydrophobic groups with a tendency to precipitate at the oil/water interface, such as polycaprolactone, as shown in Figure 4d. We demonstrate that it is also feasible to directly encapsulate undissolved oil that is previously emulsified in the ethanol solution, as modeled in Figure 4e. In the 50/50 μL mg^{-1} solution, there are some undissolved but emulsified vegetable oil droplets, as evidenced by the opaque appearance shown in Figure 4f and Figure S4, Supporting Information. When the solution containing emulsified oil droplets is quickly injected into water, all oil droplets are effectively encapsulated in the nanocapsules and the dispersion is stable for a long period of time, as shown in Figure 4g. The nanocapsules overall have a thin but relatively homogeneous shell, as shown by the SEM images in Figure 4h and Figure S5, Supporting Information. The active encapsulation of emulsified oil droplets is attributed to the preferential deposition of shellac polymer at the oil/water interface and the basic

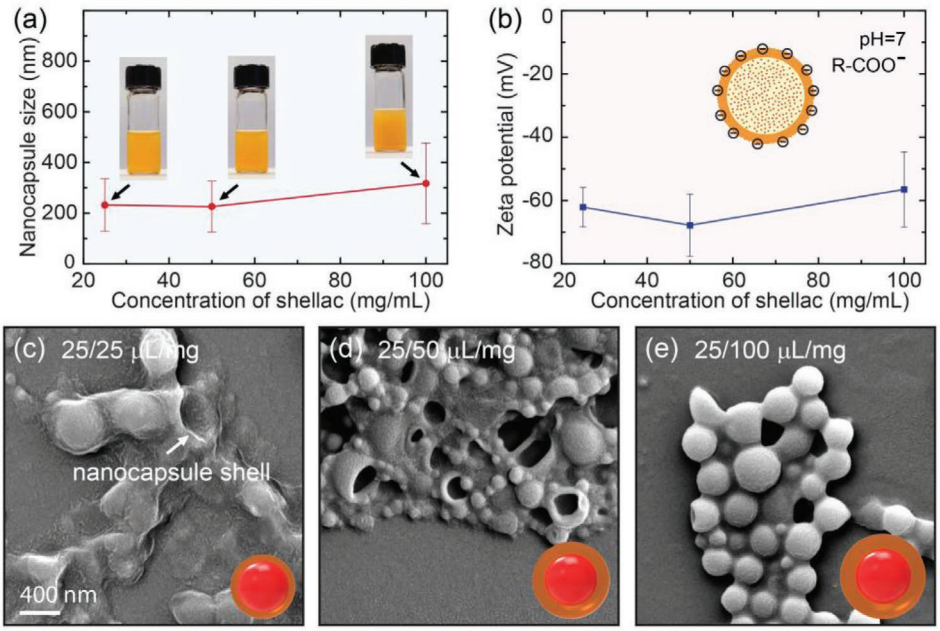

Figure 3. Flexible tailoring of the size and shell thickness of the nanocapsules. a) The size of the nanocapsules only slightly increases as the concentration of shellac polymer increases when the amount of vegetable oil is kept constant at 25 μL per mL ethanol. b) The zeta potential of the nanocapsules. SEM images of empty nanocapsules prepared by c) 25/25 μL mg^{-1}, d) 25/50 μL mg^{-1}, and e) 25/100 μL mg^{-1} solutions, showing an increase in the rigidity of the polymer shell as the shellac concentration increases. The notion 25/25 μL mg^{-1} denotes 25 μL vegetable oil and 50 mg shellac polymer per mL ethanol.

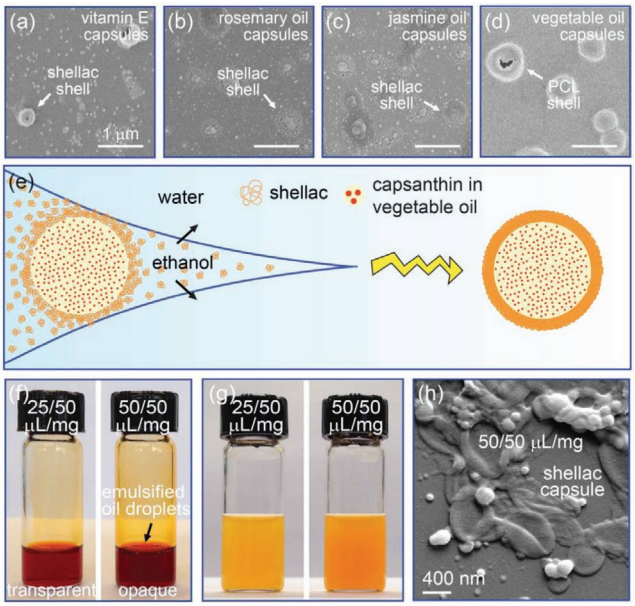

Figure 4. Active encapsulation of various oils in the biocompatible nanocapsules. SEM images showing the shellac polymer shells of a) vitamin E nanocapsules, b) rosemary oil nanocapsules, and c) jasmine oil nanocapsules and the polycaprolactone polymer shells of d) vegetable oil nanocapsules after the oil cores are removed. All the nanocapsules are prepared following the same process. e) Model of active encapsulation of oil droplets directly emulsified in the ethanol solution. f) In the 50/50 μL mg^{-1} solution, a small amount of undissolved vegetable oil is directly emulsified in the ethanol solution by vortexing, making the solution slightly opaque. g) After quickly injecting the solution into water, all oil droplets are effectively encapsulated in the nanocapsules, as evidenced by the stable dispersion. h) SEM image showing the shellac polymer shells of nanocapsules prepared by the 50/50 μL mg^{-1} solution.

principle that is applicable to various situations could solve a myriad of problems.

To determine the encapsulation efficiency, we measure the UV–vis absorption of capsanthin loaded in the nanocapsules and confirm the linear dependence of the UV–vis absorption on its concentration, as shown in Figures S6 and S7, Supporting Information. At pH = 1.6, the dissociation of H^+ cations from the carboxyl groups is strongly suppressed and the hydrophobic nature of shellac nanocapsules causes them to aggregate and settle. The portion of capsanthin left in the supernatant is regarded as the amount of unencapsulated capsanthin and we confirm that the encapsulation efficiency of the nanocapsules is as high as 98%, as calculated from the UV–vis measurements and supported by the colorless appearance of the supernatant (Figure S8, Supporting Information). The obtained encapsulation efficiency is higher than many other reported nanocapsules[46] and we attribute the high encapsulation efficiency to the controlled co-precipitation under rapid mixing and the guided nanocapsule formation by energy minimization.

The developed biocompatible nanocapsules are ideal carriers and have various advantages, including tunable shell thickness, high encapsulation efficiency, high loading capacity, and good dispersity in water. The dispersions of nanocapsules in water are stable over a wide pH range from pH = 4 to 7, as shown in **Figure 5**a and modeled in Figure 5b. Shellac polymer contains a lot of carboxylic acids, which are typical weak acids.[47] At neutral pH, the partial dissociation of the carboxyl groups at the surface makes the nanocapsules negatively charged and the electrostatic repulsion between them resists their coagulation and flocculation. At low pH, the dissociation of H^+ cations from the carboxyl groups is strongly suppressed and the hydrophobic nature of shellac nanocapsules causes them to aggregate. At high pH,

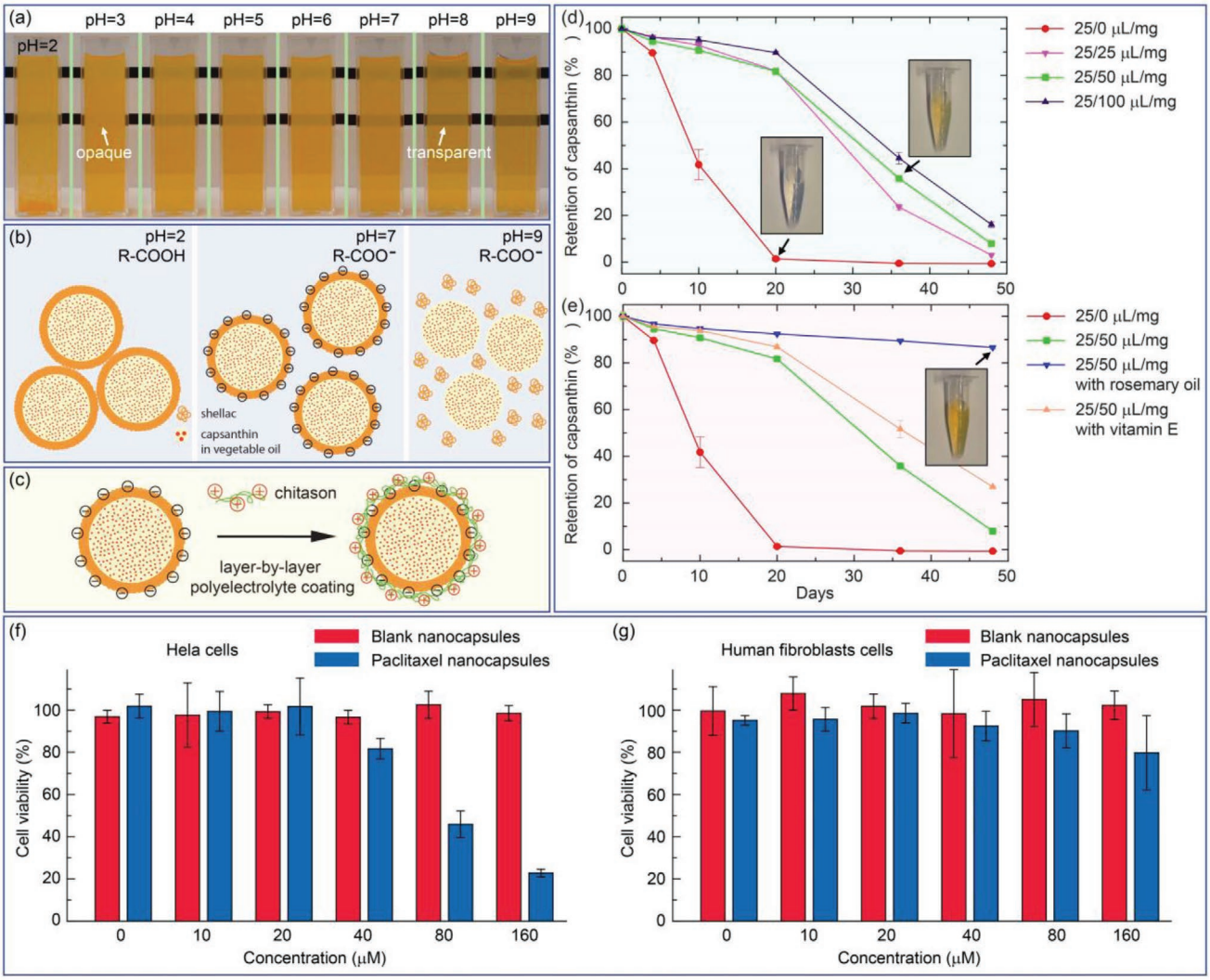

Figure 5. Dispersity and stability performances of capsanthin-loaded nanocapsules. a) The dispersion of the nanocapsules in water is stable at pH ranging from pH=4 to pH=7. b) At low pH, the dissociation of H^+ cations from the carboxyl groups is strongly suppressed and the hydrophobic nature of shellac nanocapsules causes them to aggregate. At neutral pH, the electrostatic repulsion prevents the nanocapsules from aggregation. At high pH, the high dissociation rate of the carboxyl groups makes shellac polymer dissolvable in water and the transparency of the solution increases. c) Chitosan, a positively-charged biocompatible polyelectrolyte, could revert the zeta potential of the nanocapsules from negative to positive via electrostatic interactions. d) Retention of capsanthin encapsulated in shellac nanocapsules steadily increases when the polymer shell becomes thicker. The samples are stored in dark at room temperature (≈25 °C). e) The use of natural antioxidants, for example, rosemary oil, significantly increases the stability of capsanthin. Cell viability of f) Hela and g) human fibroblast cells in the presence of blank nanocapsules (red columns) and paclitaxel-loaded nanocapsules (blue columns), suggesting that the nanocapsules are biocompatible and are ideal carriers for anti-cancer drugs.

the high dissociation rate of the carboxyl groups makes shellac polymer dissolvable in water, and the nanocapsule dispersions show an increase in transparency and a decrease in optical density, as shown in Figure S9, Supporting Information. The dissolution of shellac shells under alkaline conditions potentially provides a pH-triggered release mode for the nanocapsules. Due to the surface charges, the nanocapsules could easily be functionalized by polyelectrolyte coating. For example, the zeta potential of the nanocapsules could be reverted from –60 to 50 mV by chitosan via electrostatic interactions, as modeled in Figure 5c. These positively-charged nanocapsules are beneficial for the uptake in the gastrointestine where mucosa cells generally have a negatively-charged cell membrane.[48]

Active ingredients, such as capsanthin, are generally sensitive to light, temperature, pH, and redox agents.[49] Encapsulation of capsanthin in nanocapsules increases both its dispersity in water and stability over time, as shown in Figure S10, Supporting Information. To quantitatively demonstrate its improved stability, we monitor the fraction of undegraded capsanthin over time using UV–vis spectroscopy. In the absence of any protection, capsanthin loaded in the oil droplets is susceptible to the ambient environments and readily degrades after 20 days, as shown in Figure 5d. In contrast, capsanthin encapsulated in the nanocapsules shows a much better stability performance; about 20% capsanthin degrades after 20 days. The observed considerable reduction in degradation confirms the effective protection

of sensitive ingredients from oxidation by the polymer shell. The stability further increases when the shell thickness increases. The versatile encapsulation method allows us to add various oil antioxidants, such as vitamin E and rosemary oil, into the nanocapsules. Interestingly, the addition of a small amount of rosemary oil shows an excellent stability improvement, that is, 85% capsanthin retains after 48 days and the color of the nanocapsule suspension barely changes, as shown in Figure 5e.

The biocompatible nanocapsules could also be used as delivery vehicles of many water-insoluble drugs, which suffers from low efficacy due to poor water solubility, and avoid the use of toxic solvent or surfactant during the preparation process. Paclitaxel and doxorubicin are chosen as the model water-insoluble drugs and are encapsulated in the core–shell nanocapsules following the same procedure as capsanthin. The encapsulation efficiency of doxorubicin is confirmed to be as high as 98%, as determined by the UV–vis absorption measurements shown in Figures S11–S13, Supporting Information. The cell bioavailability of paclitaxel loaded in the nanocapsules is tested using Hela and human fibroblast cells, as shown in Figure 5f,g. The high cell viabilities of both cells cultured in the presence of blank nanocapsules suggest high cell biocompatibility of the nanocapsules. In contrast, the cell viability of Hela cells decreases dramatically as the concentration of paclitaxel loaded in the nanocapsules increases, while that of human fibroblast cells only slightly decreases, indicating that the nanocapsules could increase the bioavailability of paclitaxel and paclitaxel is less toxic to human fibroblast cells. Therefore, the results confirm that the core–shell nanocapsules are ideal carriers for drug delivery.

3. Conclusion

We develop a versatile method to prepare biocompatible nanocapsules with a delicate hierarchical core–shell structure. The controlled co-precipitation of oil and polymer under rapid mixing and the guided deposition of polymer at the oil/water interface by energy minimization ensure an effective one-step way to actively encapsulate various oils in the biocompatible nanocapsules. The core–shell nanocapsules are excellent delivery vehicles and allow the customization of cargo loading for targeted applications, such as unstable natural colorants and water-insoluble drugs. The designed ready-to-go cargo-loaded nanocapsules possess great many of advantages, including tunable shell thickness, high encapsulation efficiency, high loading capacity, good dispersity in water, enhanced stability, and improved bioavailability. The developed biocompatible nanocapsules thus represent an important step toward their practical applications.

Supporting Information

Supporting Information is available from the Wiley Online Library or from the author.

Acknowledgements

B.W. and C.Y. contributed equally to this work. This work was supported by the National Natural Science Foundation of China (Grant Nos. 21878258, 11704331, 21877104, 21834007, and 21907088), National Key R&D Program of China (2018YFA0902600), K. C. Wong Education Foundation (Grant No. GJTD-2018-09), Zhejiang University Education Foundation Global Partnership Fund and the Open Funds of the State Key Laboratory of Rare Earth Resource Utilization, Changchun Institute of Applied Chemistry, CAS (Grant No. RERU2019008). This work was also supported by the National Science Foundation (DMR1310266) and the Harvard Materials Research Science and Engineering Center (DMR-1420570). B.W. acknowledges the financial support from the China Postdoctoral Science Foundation (2019TQ0274). C.-X.Z. acknowledges the financial support from the Australian Research Council under Future Fellowship project (FT140100726).

Conflict of Interest

The authors declare no conflict of interest.

Keywords

co-precipitation, core–shell nanocapsules, encapsulation, hierarchical structures, nanocapsules

Received: April 29, 2020
Revised: May 17, 2020
Published online: June 23, 2020

[1] L. Kong, X. Jin, D. Hu, L. Feng, D. Chen, H. Li, *Chin. Chem. Lett.* **2019**, *30*, 2351.
[2] D. Liu, H. Zhang, S. Cito, J. Fan, E. Mäkilä, J. Salonen, J. Hirvonen, T. M. Sikanen, D. A. Weitz, H. A. Santos, *Nano Lett.* **2017**, *17*, 606.
[3] C. L. Mou, W. Wang, Z. L. Li, X. J. Ju, R. Xie, N. N. Deng, J. Wei, Z. Liu, L. Y. Chu, *Adv. Sci.* **2018**, *5*, 1700960.
[4] H. Zhang, Y. Zhu, L. Qu, H. Wu, H. Kong, Z. Yang, D. Chen, E. Makila, J. J. Salonen, H. A. Santos, *Nano Lett.* **2018**, *18*, 1448.
[5] G. B. Sukhorukov, A. L. Rogach, B. Zebli, T. Liedl, A. G. Skirtach, K. Kohler, A. A. Antipov, N. Gaponik, A. S. Susha, M. Winterhalter, W. J. Parak, *Small* **2005**, *1*, 194.
[6] W. Z. Zhang, M. Z. Wang, W. Tang, R. Wen, S. Y. Zhou, C. Lee, H. Wang, W. Jiang, I. M. Delahunty, Z. P. Zhen, H. M. Chen, M. Chapman, Z. H. Wu, E. W. Howerth, H. J. Cai, Z. B. Li, J. Xie, *Adv. Mater.* **2018**, *30*, 1805557.
[7] T. Zhao, P. Wang, Q. Li, A. A. Al-Khalaf, W. N. Hozzein, F. Zhang, X. Li, D. Zhao, *Angew. Chem., Int. Ed.* **2018**, *57*, 2611.
[8] W. Zhang, C. X. Wang, K. L. Chen, Y. J. Yin, *Small* **2019**, *15*, 1903750.
[9] X. L. Liang, C. Gao, L. G. Cui, S. M. Wang, J. R. Wang, Z. F. Dai, *Adv. Mater.* **2017**, *29*, 1703135.
[10] Q. Dong, X, W , X. Hu, L. Xiao, L. Zhang, L. Song, M. Xu, Y. Zou, L. Chen, Z. Chen, W. Tan, *Angew. Chem., Int. Ed.* **2018**, *57*, 177.
[11] W. H. Ji, T. L. Zhang, Z. G. Lu, J. Shen, Z. B. Xiao, X. Zhang, *Chin. Chem. Lett.* **2019**, *30*, 739.
[12] S. K. Li, J. M. Xu, S. Wang, X. Xia, L. Chen, Z. Chen, *Chin. Chem. Lett.* **2019**, *30*, 1581.
[13] Y. Li, J. Li, J. Sun, H. He, B. Li, C. Ma, K. Liu, H. Zhang, *Angew. Chem., Int. Ed.* **2020**, *59*, 8148.
[14] C. E. Mora-Huertas, H. Fessi, A. Elaissari, *Int. J. Pharm.* **2010**, *385*, 113.
[15] E. Amstad, *ACS Macro Lett.* **2017**, *6*, 841.
[16] Y. Cheng, Y. Yu, Y. Zhang, G. Zhao, Y. Zhao, *Small* **2019**, *15*, 1904290.
[17] K. Sou, D. L. Le, H. Sato, *Small* **2019**, *15*, 1900132.
[18] Y. H. Liu, Y. X. Wang, J. X. Huang, Z. X. Zhou, D. Zhao, L. M. Jiang, Y. Q. Shen, *AIChE J.* **2019**, *65*, 491.

[19] G. Z. Yang, Y. Liu, H. F. Wang, R. Wilson, Y. Hui, L. Yu, D. Wibowo, C. Zhang, A. K. Whittaker, A. P. J. Middelberg, C. X. Zhao, *Angew. Chem., Int. Ed.* **2019**, *58*, 14357.
[20] X. P. Zhang, J. Luo, D. X. Zhang, T. F. Jing, B. X. Li, F. Liu, *J. Colloid Interface Sci.* **2018**, *517*, 86.
[21] V. Nedovic, A. Kalusevic, V. Manojlovic, S. Levic, B. Bugarski, *Procedia Food Sci.* **2011**, *1*, 1806.
[22] Y. J. Surh, *Nat. Rev. Cancer* **2003**, *3*, 768.
[23] S. S. Guterres, V. Weiss, L. D. L. Freitas, A. R. Pohlmann, *Drug Delivery* **2000**, *7*, 195.
[24] W. Xu, P. A. Ledin, Z. Iatridi, C. Tsitsilianis, V. V. Tsukruk, *Angew. Chem., Int. Ed.* **2016**, *55*, 4908.
[25] C. X. Zhao, *Adv. Drug Delivery Rev.* **2013**, *65*, 1420.
[26] W. Wang, M. J. Zhang, L. Y. Chu, *Acc. Chem. Res.* **2014**, *47*, 373.
[27] M. P. Nori, C. S. Favaro-Trindade, S. M. de Alencar, M. Thomazini, J. C. de Camargo Balieiro, C. J. C. Castillo, *LWT–Food Sci. Technol.* **2011**, *44*, 429.
[28] J. Li, B. Li, J. Sun, C. Ma, S. Wan, Y. Li, R. Göstl, A. Herrmann, K. Liu, H. Zhang, *Adv. Mater.* **2020**, *32*, 2000964.
[29] Y. Luo, X. Zhou, *J. Polym. Sci., Part A: Polym. Chem.* **2004**, *42*, 2145.
[30] B. Kim, T. Y. Jeon, Y.-K. Oh, S.-H. Kim, *Langmuir* **2015**, *31*, 6027.
[31] P. D. Hede, P. Bach, A. D. Jensen, *Chem. Eng. Sci.* **2008**, *63*, 3821.
[32] T. Y. Lee, T. M. Choi, T. S. Shim, R. A. M. Frijns, S. H. Kim, *Lab Chip* **2016**, *16*, 3415.
[33] B. F. B. Silva, C. Rodríguez-Abreu, N. Vilanova, *Curr. Opin. Colloid Interface Sci.* **2016**, *25*, 98.
[34] F. N. Sang, Z. Chen, Y. D. Wang, J. H. Xu, *AIChE J.* **2018**, *64*, 730.
[35] H. Lee, C.-H. Choi, A. Abbaspourrad, C. Wesner, M. Caggioni, T. Zhu, D. A. Weitz, *ACS Appl. Mater. Interfaces* **2016**, *8*, 4007.
[36] B. F. Gibbs, S. Kermasha, I. Alli, C. N. Mulligan, *Int. J. Food Sci. Nutr.* **1999**, *50*, 213.
[37] H. Weinberger, W. H. Gardner, *Ind. Eng. Chem.* **1938**, *30*, 454.
[38] H. Matsufuji, H. Nakamura, M. Chino, M. Takeda, *J. Agric. Food Chem.* **1998**, *46*, 3468.
[39] L. Kong, R. Chen, X. Wang, C.-X. Zhao, Q. Chen, M. Hai, D. Chen, Z. Yang, D. A. Weitz, *Lab Chip* **2019**, *19*, 2089.
[40] B. K. Johnson, R. K. Prud'Homme, *Phys. Rev. Lett.* **2003**, *91*, 118302.
[41] J. M. Lim, A. Swami, L. M. Gilson, S. Chopra, S. Choi, J. Wu, R. Langer, R. Karnik, O. C. Farokhzad, *ACS Nano* **2014**, *8*, 6056.
[42] A. Loxley, B. Vincent, *J. Colloid Interface Sci.* **1998**, *208*, 49.
[43] Z. Sun, C. Yang, M. Eggersdorfer, J. Cui, Y. Li, M. Hai, D. Chen, D. A. Weitz, *Chin. Chem. Lett.* **2020**, *31*, 249.
[44] Z. Sun, C. Yang, F. Wang, B. Wu, B. Shao, Z. Li, D. Chen, Z. Yang, K. Liu, *Angew. Chem., Int. Ed.* **2020**.
[45] L. Kong, E. Amstad, M. Hai, X. Ke, D. Chen, C.-X. Zhao, D. A. Weitz, *Chin. Chem. Lett.* **2017**, *28*, 1897.
[46] N. V. N. Jyothi, P. M. Prasanna, S. N. Sakarkar, K. S. Prabha, P. S. Ramaiah, G. Srawan, *J. Microencapsulation* **2010**, *27*, 187.
[47] D. Chen, E. Amstad, C.-X. Zhao, L. Cai, J. Fan, Q. Chen, M. Hai, S. Koehler, H. Zhang, F. Liang, *ACS Nano* **2017**, *11*, 11978.
[48] M. H. El-Shabouri, *Int. J. Pharm.* **2002**, *249*, 101.
[49] T. Philip, F. Francis, *J. Food Sci.* **1971**, *36*, 96.